

# SCIENTIFIC RESEARCH

Scientific Report No. 77

## SUPERSONIC AND SUBSONIC MEASUREMENTS OF MESOSPHERIC IONIZATION

by  
J. H. ...

The results of the measurements of the ionization of the mesosphere at supersonic and subsonic speeds are presented in this report. The measurements were made at the ...

### PLASMA RESEARCH LABORATORY

740177  
PSU - IRL - SCI 377

Scientific Report 377

"Supersonic and Subsonic Measurements of Mesospheric Ionization"

by

Larry Nickell

November 1, 1971

"The research reported in this document has been sponsored by the Department of the Army, Army Research Office-Durham under Grant DA-ARO-D-31-124-71-G110 and in part by the National Science Foundation under grant GZ-1708.

Submitted by:

Leslie C. Hale

Leslie C. Hale, Professor of Electrical  
Engineering, Project Supervisor

Approved by:

John S. Nisbet  
John S. Nisbet, Director  
Ionosphere Research Laboratory

Ionosphere Research Laboratory  
The Pennsylvania State University  
University Park, Pennsylvania 16802

## ACKNOWLEDGEMENTS

The guidance of Dr. L. C. Hale is sincerely appreciated. I would also like to acknowledge the assistance of the personnel of White Sands Missile Range, New Mexico and the Ionosphere Research Laboratory of The Pennsylvania State University.

TABLE OF CONTENTS

	Page
ACKNOWLEDGEMENTS . . . . .	i
LIST OF FIGURES . . . . .	iii
ABSTRACT. . . . .	iv
INTRODUCTION . . . . .	1
1.1 Statement of the Problem . . . . .	1
1.2 Scope of this Work . . . . .	2
THEORETICAL DEVELOPMENT . . . . .	4
2.1 Background . . . . .	4
2.2 Theory for a D-region Experiment . . . . .	4
DESCRIPTION OF THE INSTRUMENT . . . . .	8
3.1 Experiment Implementation . . . . .	8
3.2 Design . . . . .	8
EXPERIMENTAL RESULTS . . . . .	15
4.1 Flight History. . . . .	15
4.2 Data Analysis. . . . .	15
4.2.1 Nose-Tip. . . . .	15
4.2.2 Blunt Probe . . . . .	20
OBSERVATIONS AND INTERPRETATIONS . . . . .	22
5.1 Comparison of Data . . . . .	22
5.2 Interpretations . . . . .	24
CONCLUSION . . . . .	25
REFERENCES. . . . .	27

LIST OF FIGURES

Figure		Page
1	Electric Field Versus Applied Voltage for Blunt and Nose-Tip Probe . . . . .	7
2	Nose-Tip Probe . . . . .	9
3	Electrometer Equivalent Circuit with Parasitic Capacitance . . . . .	11
4	Mach Number Versus Altitude for Blunt and Nose-Tip Probe . . . . .	17
5	Typical Nose-Tip Data Block . . . . .	18
6	Example of $E/P_0$ Dependence at 79 km. . . . .	19
7	Conductivity Versus Altitude for Blunt and Nose-Tip Probe . . . . .	23

## ABSTRACT

An Arcas rocket-parachute system was used at night to compare supersonic and subsonic ionization measurements below 75 km. A hemispherical nose-tip probe was used on ascent and a parachute-born blunt probe was employed on descent to measure polar conductivities, which were due entirely to positive and negative ions. The velocity of the supersonic probe was  $\sim$ Mach 2.5 at 50 km. and 1.75 at 70 km.; the blunt probe was subsonic below 71 km.

Between 65 and 75 km. the ratio of negative to positive conductivities (and thus of mobilities) determined by the blunt probe was about 1.2, and it approached 1 below this altitude range. The ratio obtained by the nose-tip varied from 1.5 at 75 km. to .6 at 65 km., thus indicating a rapid variation of the effects of the shock wave on the sampled ions.

The absolute values of positive conductivity measured subsonically and supersonically were essentially identical from 60 to 75 km., indicating that the sampled ions were unchanged by the shock. However, below 60 km. the shock apparently "broke-up" the positive ions, as indicated by higher measured conductivities.

The negative ion conductivities for the supersonic case indicated a very divergent effect of the shock. The negative ions were apparently lighter (higher mobility) than those sampled subsonically above 72 km. and below 50 km. However, they appeared heavier (lower mobility) at the intervening altitudes.

## INTRODUCTION

### 1.1 Statement of the Problem

The use of simple blunt metal probes to measure upper atmospheric ionic conductivities in the continuous regime of operation, typically below 80 km., has been discussed by several authors. Hoult (1) discussed subsonic probes and concluded that under certain conditions such probes will collect ions according to a simple mobility theory, independent of angle of attack and other flow variables. A more general theory was proposed by Sonin (2) in which he extended this result to supersonic probes. However, there is still uncertainty as to whether the basic assumptions of this theory apply to a supersonic experiment in the D-region. This is because the effects of flow variables, particularly the shock wave, upon the gas surrounding the probe are not fully understood. This is especially true when considering the effects upon the chemical structure of the gas.

This uncertainty is greatly reduced for the subsonic case due to the absence of flow effects and the shock wave. Consequently, subsonic measurements in the ionosphere are probably preferable when it is practical to use them. The most practical method for accomplishing this is the use of a rocket-launched parachute-borne payload deployed near the apogee of the rocket trajectory, because of the exponentially rapid variation of atmospheric density with altitude. The altitude range one wishes to measure with a subsonic probe will determine the size of payload and parachute needed, with the size of parachute increasing very rapidly with payload weight and

design and theoretical development of this nose-tip is shown. A brief history and discussion of supersonic flow theory is also contained here.

Two of these supersonic experiments have been performed on an Arcas launched rocket-parachute systems at White Sands Missile Range. The data analysis and subsequent comparison are contained in this work. A discussion of this comparison and its implications is also given.

## THEORETICAL DEVELOPMENT

### 2.1 Background

As cited by Richards (3), Langmuir established the basis of modern probe theory in the late twenties. However, Langmuir confined himself mainly to low pressure and collisionless problems. This is not the case for the altitudes below 75 km. considered herein. Consequently, classical probe theory cannot be applied to this experiment. Hoult (1) has shown that subsonic probes of sufficiently blunt geometry can collect charge by a simple mobility mechanism independent of angle of attack. Slender body geometries, such as the Gerdien condenser, disturb the environment less but are much more sensitive to angle of attack, the angle between the probe axis and the trajectory tangent. The Gerdien condenser is theoretically capable of providing both number density and conductivity information. However, such experiments are fairly difficult to perform, particularly subsonically. This is mainly due to the difficulty of maintaining a low angle of attack.

The research reported here is directed toward implementing a simpler supersonic blunt probe (nose-tip) to produce the simplest possible system capable of providing useful synoptic information. The theory used for this experiment was developed by Sonin (2). His work is an extension of subsonic blunt probe theory and is independent of angle of attack and flow effects under certain conditions.

### 2.2 Theory for a D-region Experiment

As previously mentioned, the theory developed by Sonin (2) is used for this supersonic experiment. Sonin's theory concludes that,

in the strong field limit, the particle collection will be dominated by the electric field drift. Sonin's theory yields a collection rate equation which is essentially the same as that of the subsonic probe. The assumptions on which Sonin bases his conclusions are:

- 1) Flow Reynolds number  $\gg 1$
- 2) Weakly ionized gas
- 3)  $(\gamma_D/R)^2 \gg kT/eV$
- 4) Chemically frozen flow

where, for 3), R represents a characteristic length of the probe, V the applied potential, e the electron charge and  $\gamma_D$  the Debye length. The first three assumptions are readily met, but Keller (4) has pointed out that the fourth assumption is almost certainly not true, even in the subsonic case. However, the way assumption four enters into the theory is such that chemical reactions will not greatly effect measured conductivity if they only involve ion-molecule charge transfer reactions which do not greatly alter ionic mobility. Then a properly chosen average mobility will enable the conversion of measured conductivities to number densities.

The criteria for a strong field (E) is

$$E > - \frac{2}{Zi} (4 S_{cio} Re)^{1/2}$$

where  $S_{cio}$  is the Schmidt number evaluated at free stream conditions, Re the Reynolds number based on stagnation conditions and eZi the particle charge. However, as cited by Keller (4), the inequality

$$\frac{E}{P_o} < 2 \text{ V/Cm - mmHg}$$

where  $P_0$  is the local pressure, must hold for mobility to remain essentially constant. Mobility must remain constant in order for conductivity to be reduced to number density. The electric field for the nose-tip and blunt probe is shown in Figure 1. The nose-tip field is within the boundaries set forth above except at the higher altitudes (79 km.) where  $E/P_0$  is greater than two. This point is discussed later.

As will be shown, the nose-tip collector configuration is a hemisphere. Therefore, an equation for the probe electric field can be found by solving Laplace's equation in spherical co-ordinates. Doing this, we have

$$\vec{E} = \frac{aV}{R^2} \hat{a}_R$$

where  $a$  is the sphere radius and  $V$  the applied potential. The current collected by the probe is

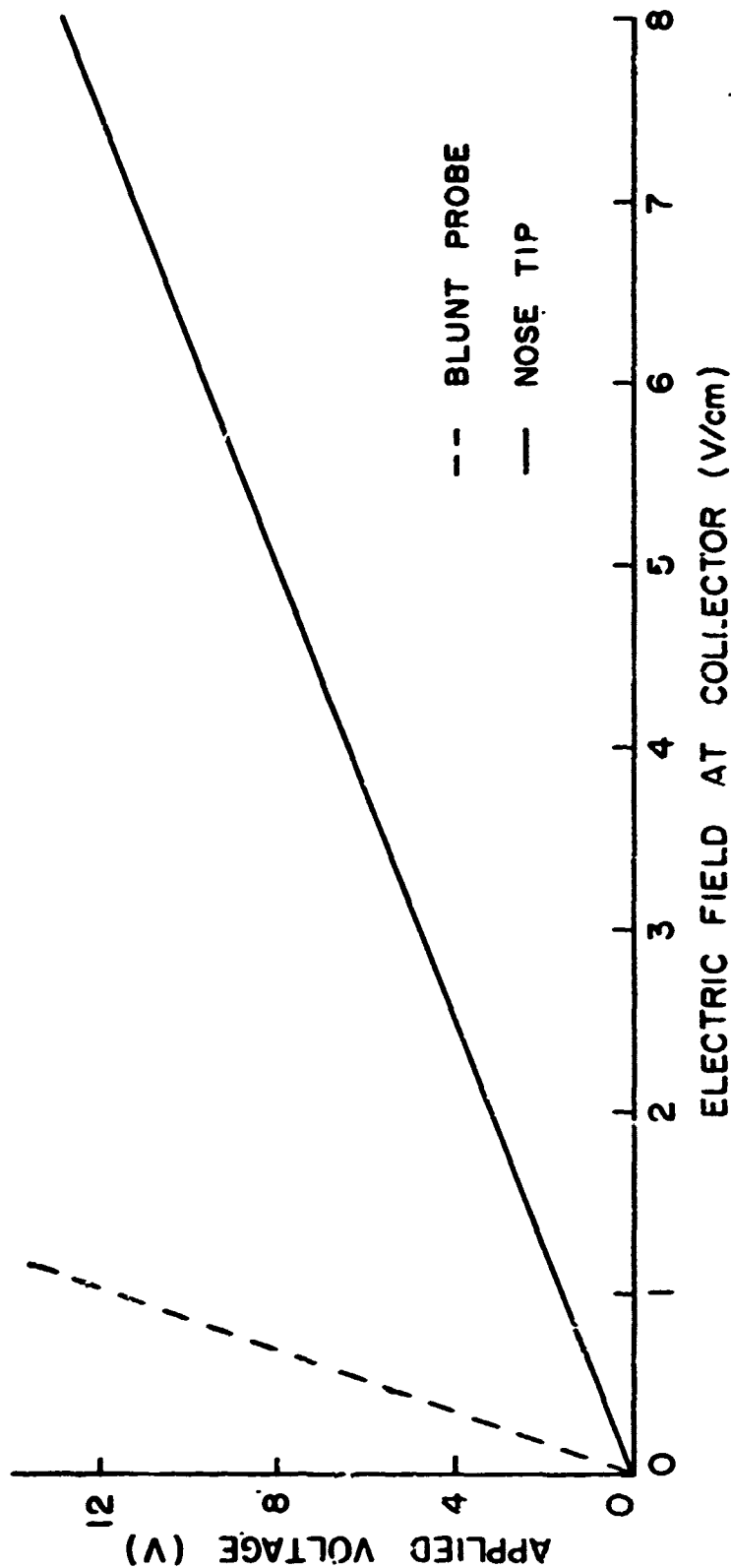
$$I_+ = J_+ A = \sigma_+ E_- A$$

$$I_- = J_- A = \sigma_- E_+ A$$

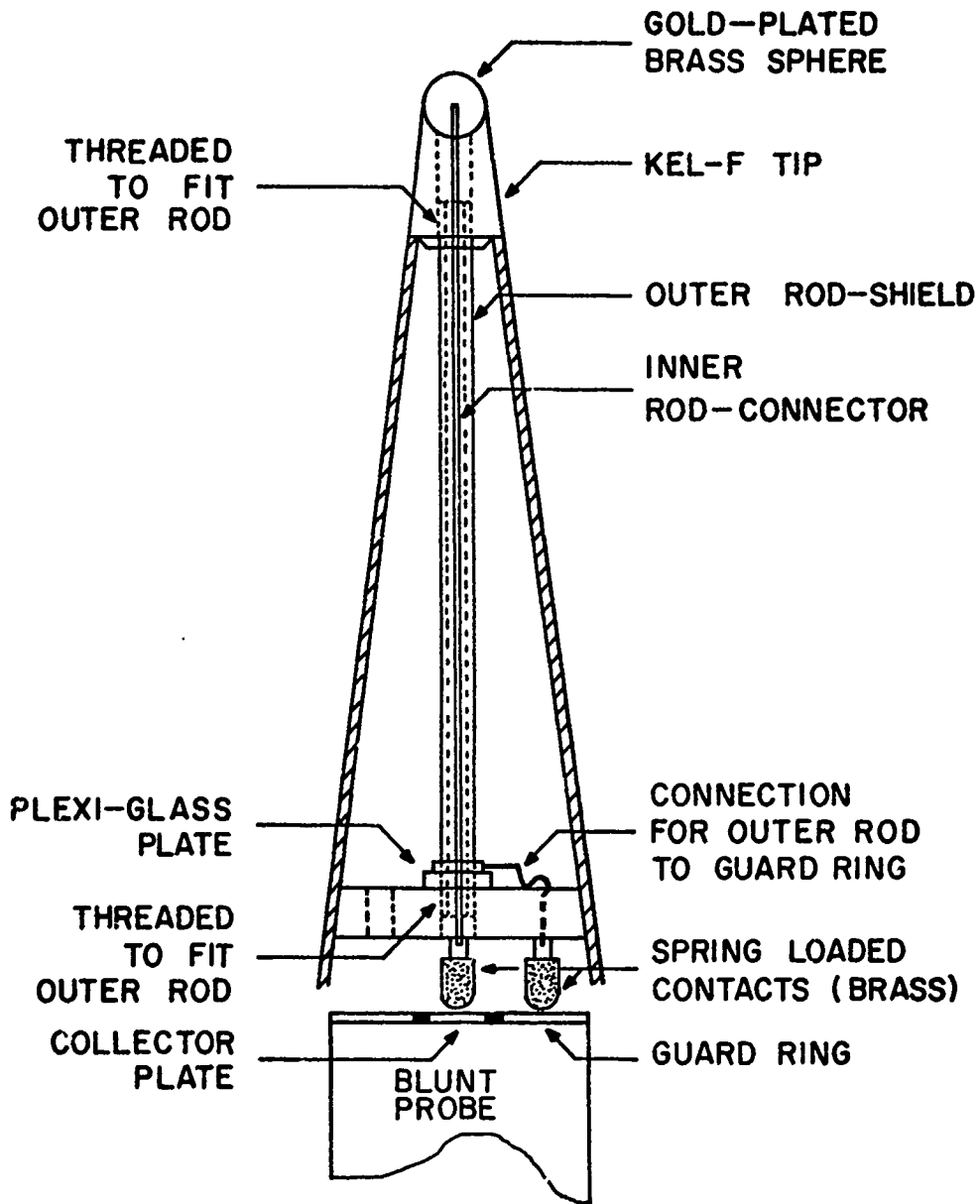
where  $\sigma_+$  and  $\sigma_-$  are the medium polar conductivities,  $E_-$  and  $E_+$  are the fields at a negative and positive probe surface, respectively, and  $A$  is the collecting surface area. This results in the collection rate equation

$$I_{\pm} = 2\pi aV \sigma_{\pm}$$

where  $\sigma_{\pm}$  will heretofore denote the polar conductivities.



ELECTRIC FIELD VERSUS APPLIED VOLTAGE FOR BLUNT AND NOSE TIP PROBE  
FIGURE I



NOSE TIP PROBE  
FIGURE 2

A circuit equivalent of the electrometer with this capacitance is shown in Figure 3. Where the current source (I) replaces the current due to the collected ions,  $R_f$  is the feedback resistor for the operational amplifier,  $R_c$  the calibration resistor,  $-k$  the amplifier gain and  $C$  the co-axial capacitance element. Simple classical analysis of a co-axial line shows the capacitance per unit length to be

$$\frac{C}{l} = 2\pi \epsilon / \ln \left( \frac{b}{a} \right)$$

where  $b$  is the radius to the outer conductor,  $a$  the radius of the inner conductor,  $l$  the length of the rod and  $\epsilon$  the permittivity of the insulation. For the insulation used (Belden shrinkable tubing), the dielectric constant is 2.65. Thus, knowing the values of  $a$ ,  $b$ ,  $l$ , and  $\epsilon$ , the total input capacitance found is

$$C = 26 \text{ pfd}$$

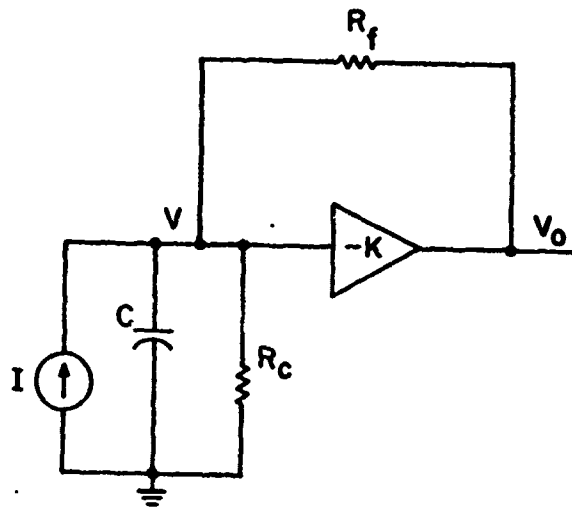
The main effect of this capacitance is upon frequency response. Referring to Figure 3, it is possible to write two equations to describe this circuit. First, a node equation at  $V$  will give

$$I = \frac{V_o - V}{R_f} + \frac{V(1 + sR_c C)}{R_c}$$

where  $s = j\omega$ . Also, across the amplifier we have

$$V_o = -kV$$

Solving these two equations simultaneously and rearranging the result will give the following transfer function



ELECTROMETER EQUIVALENT CIRCUIT WITH  
PARASITIC CAPACITANCE  
FIGURE 3

$$\frac{V_o}{I} = \frac{-R_f}{\frac{R_f}{kR_c} + 1 + j\omega \frac{R_f C}{k}}$$

The response of this system will be down 3db when the real and imaginary parts of the denominator of the above transfer function are equal. Therefore, we have

$$f_c = \frac{1}{2\pi R_f C} \frac{R_f + R_c k}{R_c}$$

for the upper cutoff frequency. Typical values for the elements in this circuit are:  $R_f = 2 \times 10^{11} \Omega$ ,  $R_c = 10^{12} \Omega$ , and  $k = 1000$ . Using these, the upper cutoff frequency was found to be

$$f_c = 36.6 \text{ Hz}$$

The sweep waveform used for this experiment has a frequency of .1 Hz. Therefore, the addition of the parasitic capacitance across the input of the probe should not effect the data.

The top of the outer conductor of the co-ax is threaded to match a Kel-f tip which encases the metal collector. When the tip is threaded on the rod, the bottom plexiglass plate is pulled up tight against the nose cone walls. Due to the irregularity of these walls, it is impossible to machine the bottom plate to fit every nose cone such that the brass plungers will make correct contact with the blunt probe when assembled. Consequently, the plate is machined smaller than necessary and layers of tape are applied around the edges. The springs in the plungers allow one quarter of an inch movement and, as a result, using tape to place to bottom plate correctly is not difficult. Two holes are also drilled in this plate to prevent

formation of a pressure differential. However, it is believed that the air leakage into the cone is negligible. This is because the tip base is sloped so as to press against the edges of the nose cone and form a seal. Kel-f was chosen as material for this tip because of its thermal properties and chemical inertness.

The inner conductor protrudes from the tip and is threaded to match the metal collector. This collector is a gold-plated brass sphere and it is half exposed to the medium. It was gold-plated to facilitate cleaning and prevent oxidization of the surface.

This probe assembly is very easy to assemble and is inexpensive. This design, on a smaller scale, will lend itself very well to construction of a complete probe to be used with standard parachute units. That is, the essential electronics can be mounted on top of the plexiglass plate and the power and telemetry connections can be made below it. However, the main point of the design is that the blunt probe can be deployed for its usual subsonic mode of operation after apogee. This enables one to obtain subsonic and supersonic data from one rocket flight. Comparison of these two different systems is, of course, the ultimate goal.

The theory and practice of blunt probe measurements have been summarized by Hale, Hault and Baker (5) and the probe used here employs the same principles. Briefly, ions are collected by a symmetrical voltage waveform that is swept linearly between the collector and a return electrode. For the subsonic case, the return electrode is the probe case and, for the supersonic case, it is the rocket body. The collected ion current is measured by an

electrometer which as a voltage output which varies as the collected current varies. This electrometer output controls a VCO which can vary between zero and two hundred Hz. for an input voltage variation of zero to plus ten volts. The VCO output turns a transmitting tube on and off at the varying frequency. Correlation between this changing frequency and the value of collected current is done by calibrating system with a known resistance in place of the medium.

The collection rate equation for the blunt probe is

$$I_{bp} = \sigma \frac{r^2}{R} V$$

where  $\sigma$  is the medium conductivity and  $R$  and  $r^2$  are the guard ring and collector disc radii, respectively. To divide this equation into the collection equation for the nose-tip would give the sensitivity of one compared to the other. Therefore, the ratio is

$$\frac{I_{nt}}{I_{bp}} = 2\pi a \frac{R}{r^2}$$

Using proper values for the actual physical dimensions gives

$$\frac{I_{nt}}{I_{bp}} = 10$$

Therefore, the nose-tip is ten times more sensitive than the blunt probe. This causes difficulties because of the saturation limit of the electrometer. Experiment has shown this arrangement to work well at night but not during the day when there is a much higher electron density.

## EXPERIMENTAL RESULTS

### 4.1 Flight History

Two of the supersonic-subsonic payloads have been flown on Arcas rockets at White Sands Missile Range. The first experiment was performed during the day and no supersonic data was received due to the excessive sensitivity of the probe. The second experiment was performed on October 13, 1970 at 2020 MST. The following discussion of data is limited to this flight.

### 4.2 Data Analysis

#### 4.2.1 Nose-Tip

The pulse position data received from the probe is a function of the current collected by the nose-tip. This functional relationship is found by placing a calibration resistor at the electrometer input and sweeping the voltage at that point. That is, the sweep voltage is applied across the calibration resistor rather than across the collector and return electrode. From the data received in the calibration mode of operation, one can determine the value of current that corresponds to a particular value of data frequency. However, it is easier and more accurate to relate slopes of current and voltage rather than discrete points. Thus, the voltage sweep is a sloping waveform. Consequently, the following data reductions will deal with rates of change.

As previously stated, the nose-tip collection equation is:

$$I_{\pm} = 2\pi a V \sigma_{\pm}$$

Dealing with rates of change of current and voltage, the medium conductivity is

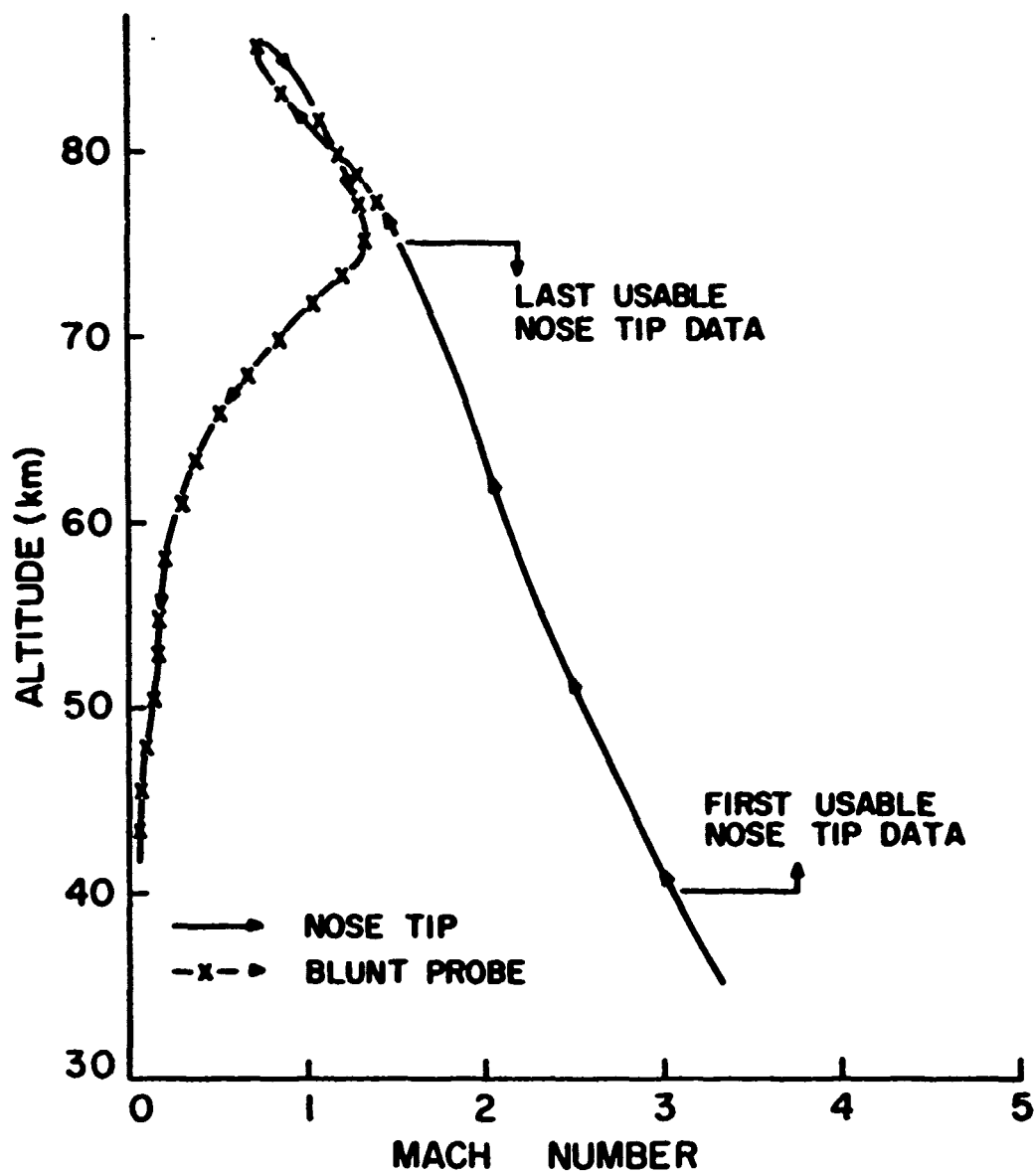
$$\sigma_{\pm} = \frac{1}{2\pi a} \frac{\Delta I}{\Delta V}$$

Putting this in a form which is more easily applied to data reduction, we have

$$\sigma_{\pm} = \frac{1}{2\pi a} \frac{1}{R_c} \left| \frac{\Delta f}{\Delta t} \right|_{\text{cal}}^{-1} \left| \frac{\Delta f}{\Delta t} \right|_{\text{data}}$$

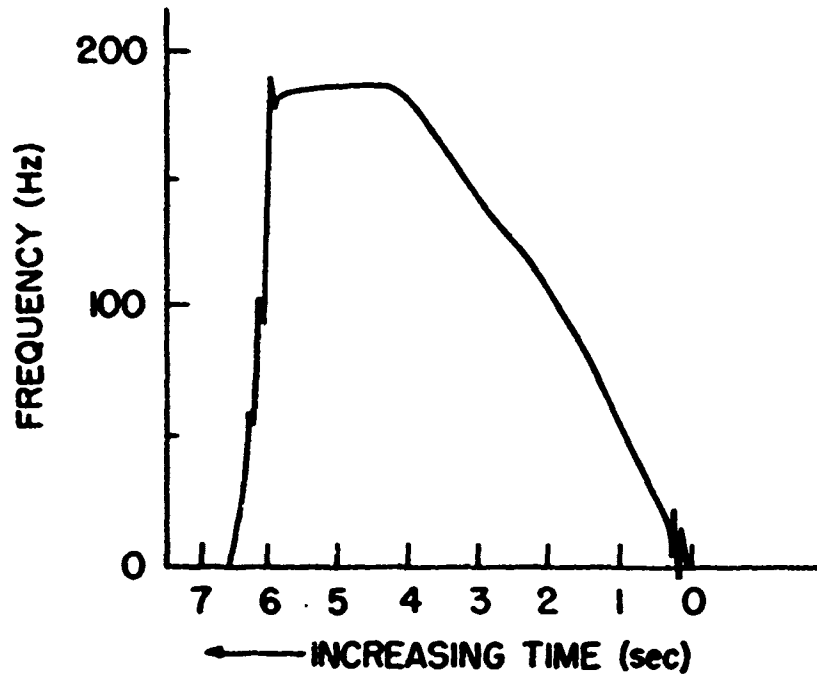
where  $R_c$  is the calibration resistor,  $\left| \frac{\Delta f}{\Delta t} \right|_{\text{cal}}$  is the slope of the frequency-time curve during the calibration mode of operation, and  $\left| \frac{\Delta f}{\Delta t} \right|_{\text{data}}$  is the equivalent during the flight mode of operation. This is a convenient form as the received data is actual VCO output. This output can be displayed graphically such that the data and calibration slopes can be measured directly.

An important parameter which can be found for this flight is Mach number. Figure 4 shows Mach number versus altitude for the nose-tip and blunt probe. Good data was received when the Mach number fell below three. A typical data block is shown in Figure 5. As can be seen, the slopes are very well behaved and linear. There is no deviation near the origin where the electric field is low. The  $E/P_0$  dependence appeared once at 79 km. This is shown in Figure 6. Notice that as the electric field approaches its maximum, the slope increases greatly. As cited by Keller (4), this is when the particles begin to acquire more energy between collisions than they lose during the collisions.

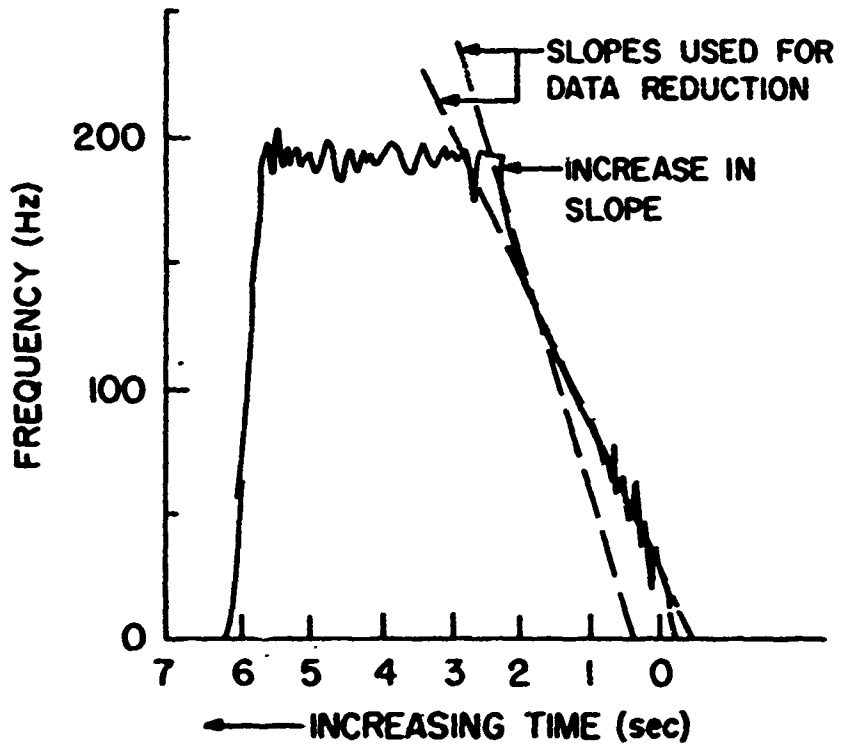


**MACH NUMBER VERSUS ALTITUDE FOR BLUNT AND NOSE TIP PROBE**

**FIGURE 4**



TYPICAL NOSE TIP DATA BLOCK  
FIGURE 5



EXAMPLE OF  $E/P_0$  DEPENDENCE AT 79 km  
FIGURE 6

#### 4.2.2 Blunt Probe

The blunt probe data analysis did not deviate from that set forth previously and the work done in the past by Baker (7). However, it should be noted that this data was corrected for night conditions. That is, at night the exact collection equations for positive and negative ion currents are

$$I_C^+ = \sigma_+ (r^2/R) V \left[ 1/(1 + \alpha \gamma) \right]$$

$$I_C^- = \sigma_- (r^2/R) V \left[ 1/(1 + \gamma/\alpha) \right]$$

where  $r$ ,  $R$ ,  $V$  and  $\sigma_{\pm}$  have the same previous definitions,  $\alpha$  is equal to  $\sigma_+/\sigma_-$ , and  $\gamma$  is equal to  $L_p/L_r$ , a dimensionless ratio of length parameters. For the night shot considered,  $\gamma = .465$  and  $\alpha$  varied as  $\sigma_+$  and  $\sigma_-$  varied. These additional factors cause  $\sigma_{\pm}$  to change by as much as 1.5. To give an exact conductivity, this process is iterative. That is, when one determines a new conductivity, he should go back and recalculate  $\alpha$ . This value of  $\alpha$  will give a more accurate conductivity profile. This recalculation process will rapidly converge to proper conductivity values. For the present case,  $\alpha$  was recalculated twice and a reasonably accurate conductivity profile was obtained.

Past work has indicated that the orientation of a subsonic probe is very uncertain immediately after ejection (9). The speed of this particular payload was found to be supersonic at the higher altitudes even though parachute deployment here is quite certain.

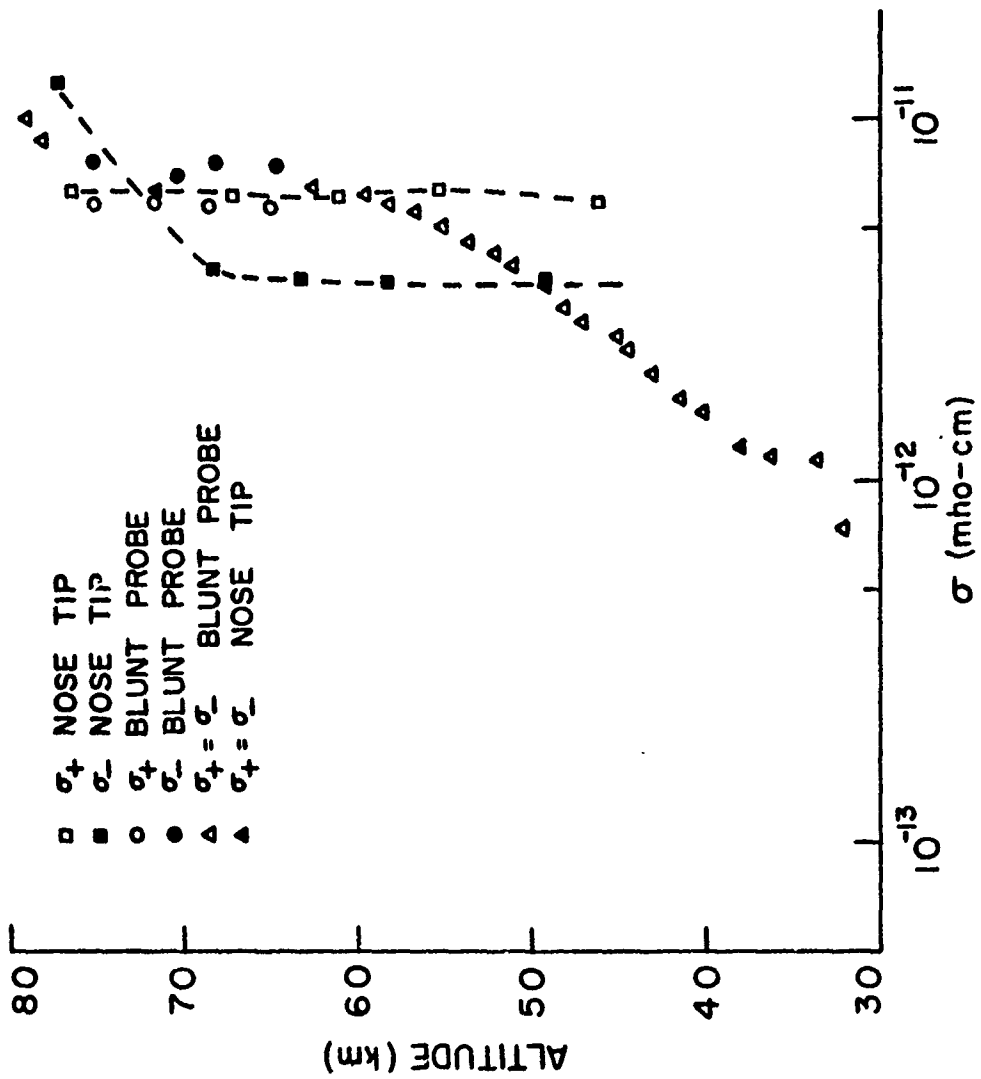
The reduced data for this top region was not consistent with past experience or internally consistent. Therefore it is believed that the speed and orientation factors are responsible for this behavior. This high altitude data is not presented here.

## OBSERVATIONS AND INTERPRETATIONS

### 5.1 Comparison of Data

The altitude range from 47 km. to 75 km. is valid for a comparison of supersonic and subsonic data. Figure 7 shows the conductivity plot for this altitude range. It will be noticed that the positive conductivity measured by the nose-tip remains essentially constant for the entire range considered. Between 55 km. and 75 km. these values essentially agree with those measured by the blunt probe. However, below 55 km. the nose-tip deviates by a maximum factor of 2.4 from the subsonic measurements. As previously mentioned, the supersonic nose-tip is less ideal than the subsonic experiment. Consequently, a possible conclusion is that it is difficult to go wrong in measuring positive ion conductivity in the 55 to 75 km. region by simply applying the Hoult-Sonin mobility theory.

The negative conductivities measured by the nose-tip are a factor of two smaller than the blunt probe measurements from 55 to 70 km. Above this range the nose-tip negative conductivity merges toward the blunt probe values and then exceeds them. It is interesting to note the crossover of nose-tip data at 71 km. Up to this point  $\sigma_- > \sigma_+$ , which is contrary to the subsonic data. The Mach number at this point is 1.65. A similar behavior and crossover was noted in the blunt probe data at 78 km. The Mach number at this crossover is 1.5.



CONDUCTIVITY VERSUS ALTITUDE FOR BLUNT AND NOSE TIP PROBE  
FIGURE 7

## 5.2 Interpretations

Since  $\sigma_{\pm} = ne\mu$ , where  $n$  is number density,  $e$  electron charge, and  $\mu$  mobility, the ratio of nose-tip to blunt probe conductivities would be a ratio of mobilities of the particles measured by the different systems. This is in direct consequence of Sonin's theory which gives the collection equation in terms of free stream density and mobility.

Looking at this ratio for positive ions up to 55 km., we see that the supersonic ions have a higher apparent mobility than that inferred from the blunt probe. This higher mobility indicates that the nose tip collected a lighter ion than did the blunt probe. Of course, from 55 km. and up, the conductivity ratio is unity and the blunt probe and nose-tip "see" the same ion mobility.

On the other hand, between 55 km. and 70 km., the conductivity ratio for negative ions indicates that the nose-tip measures a lower mobility ion than does the blunt probe. This implies that the nose-tip collects a heavier ion than the blunt probe for the same altitude range. Above this range, the ratio shows that the nose-tip collected negative ion goes from heavier to lighter than the ion collected by the blunt probe.

## CONCLUSION

Sonin supports his assumption of chemically frozen flow by showing that most reactions are too slow, in comparison with  $R/V_{\infty}$ , where  $V_{\infty}$  is the vehicle speed, to affect the constituents of the current collected. However, the present nose-tip data below 60 km. indicates that chemical reactions are taking place behind the shock wave and that these reactions are altering the apparent mobility of the ions collected. This conclusion, relating to chemical reactions, is supported by looking at nose-tip and blunt probe data below 60 km. Here the blunt probe measures the conductivity of negative and positive ions to be the same. However, the nose-tip probe shows two very different conductivities for positive and negative ions below 60 km. In their recent experiments, Rose and Widdel (9) found two positive and one negative ion in the altitude range from 72 to 58 km. One of the positive ions was a very light ion having eight times the extrapolated reduced mobility of ground level ions. The other positive ion was a heavier, aerosol particle which was four times less mobile than the extrapolated ground level ion. The negative ion measured by Rose and Widdel had about the same mobility as the lighter positive ion. The presence of the heavy positive ion may increase the chances of chemical reactions affecting the measured current. Most probably, the shock wave is breaking up this heavy ion to produce the effects seen in the nose-tip data. However, it is impossible to derive free stream information from the nose-tip data given here because the exact reaction or elements involved are unknown.

Above 60 km., the supersonic positive ion data is very much the same as the subsonic data. Thus, as mentioned before, it is probably difficult to go wrong measuring positive ions in the 60 to 75 km. range by simply using the Hault and Sonin theory. However, negative ions in this range are a different case. Here, the nose-tip shows a heavier negative ion than does the blunt probe. This seems to indicate that the shock is causing a reaction which produces a heavier ion. The nature of the positive aerosol ion is not known, and it is possible that this ion is also producing this observed behavior. That is, if the heavy positive ions were a cluster of positive and negative ions, the lower Mach number above 60 km. may not cause all of this ion to break up. This is supported by the fact that as the Mach number decreases, the conductivity measured by the nose-tip merges with the blunt probe. However, the exact reactions and elements involved must be known before one can reach a definite conclusion about the negative ions : bove 60 km.

REFERENCES

- (1) D. P. Hault, *J. Geophys. Res.*, 70 (1965), 3183.
- (2) A. A. Sonin, *J. Geophys. Res.*, 72 (1967), 4547.
- (3) E. N. Richards, *Positive Ion Densities from a Rocket Borne Hemispherical Langmuir Probe: 40 to 100 km.*, Space Data Analysis Laboratory, Department of University Research, Boson College, 1970.
- (4) G. E. Keller, *J. Geophys. Res.*, 73 (1968), 3483.
- (5) L. C. Hale, D. P. Hault, and D. C. Baker, *Space Research VIII* (North-Holland, Amsterdam, 1968), p. 320.
- (6) E. W. McDaniel, Collision Phenomena in Ionized Gases, 1964, Chapter 9.
- (7) D. C. Baker, *Ionospheric D-Region Parameters from Blunt Probe Measurements During a Solar Eclipse*, Ionosphere Research Laboratory, The Pennsylvania State University, Scientific Report No. 334, 1969.
- (8) J. W. Bond, K. M. Watson, and J. A. Welch, Atomic Theory of Gas Dynamics, 1965, p. 25.
- (9) H. U. Widdel, G. Rose, and R. Borchers, *Results of Concentration and Mobility Measurements of Positively and Negatively Charged Particles taken by a Rocket-Borne Parachute Aspiration (Gerdien) Probe in the Height Region from 72 to 39 km.*, PAGEOPH 84, pp. 154-160, 1971.
- (10) L. C. Hale, *A Probe Assembly for the Direct Measurement of Ionospheric Parameters*, Ionosphere Research Laboratory, The Pennsylvania State University, Scientific Report No. 223 (E), 1964.